

Valence study of $\text{Li}(\text{Ni}_{0.5}\text{Mn}_{0.5})_{1-x}\text{Co}_x\text{O}_2$ and $\text{LiNi}_{1-x}\text{Co}_x\text{O}_2$: The role of charge transfer and charge disproportionation

Daisuke Takegami ^{1,2}, Kosuke Kawai ³, Miguel Ferreira-Carvalho ^{4,2}, Sahana Rößler ², Cheng-En Liu,⁵
Chang-Yang Kuo,^{2,5,6} Chun-Fu Chang ², Atsusa Minamida,³ Tatsuya Miyazaki,³ Masashi Okubo,³
Liu Hao Tjeng ² and Takashi Mizokawa ¹

¹Department of Applied Physics, Waseda University, Shinjuku, Tokyo 169-8555, Japan

²Max Planck Institute for Chemical Physics of Solids, Nöthnitzer Straße 40, 01187 Dresden, Germany

³Department of Electrical Engineering and Bioscience, Waseda University, Shinjuku, Tokyo 169-8555, Japan

⁴Institute of Physics II, University of Cologne, Zùlpicher Straße 77, D-50937 Cologne, Germany

⁵Department of Electrophysics, National Yang Ming Chiao Tung University, Hsinchu 30010, Taiwan

⁶National Synchrotron Radiation Research Center, 101 Hsin-Ann Road, Hsinchu 30077, Taiwan



(Received 4 October 2023; revised 7 February 2024; accepted 18 April 2024; published 7 May 2024)

The series of LiMO_2 (M : transition metal) materials are highly relevant as cathode materials of Li-ion batteries. The stability of such systems remains an important factor for their usability in batteries, and depends strongly on the electronic configuration of the transition-metal ions. In particular, the promising class of multi-transition-metal systems exhibits complicated valence states due to intermetallic charge transfer and charge disproportionation. Here we perform a systematic study on the valence of the transition-metal ions using x-ray absorption spectroscopy on the M - $L_{2,3}$ edges and O- K edges. In $\text{Li}(\text{Ni}_{0.5}\text{Mn}_{0.5})_{1-x}\text{Co}_x\text{O}_2$ we established that the valence is Co^{3+} and $\text{Ni}_{0.5}^{2+}\text{Mn}_{0.5}^{4+}$ throughout the whole series. Meanwhile, in $\text{LiNi}_{1-x}\text{Co}_x\text{O}_2$ we found that the Ni displays a behavior consistent with a charge disproportionated negative charge transfer system, and that with increased concentration of Co^{3+} , the disproportionation signal decreases. Since the number of O $2p$ holes also gets reduced, we infer that the material will also become more unstable.

DOI: [10.1103/PhysRevMaterials.8.055401](https://doi.org/10.1103/PhysRevMaterials.8.055401)

I. INTRODUCTION

Layered transition-metal oxides LiMO_2 (M : transition metal) are widely used as cathode materials for Li-ion-based rechargeable batteries. In general, LiMO_2 has α - NaFeO_2 structure (rhombohedral system, space group $R\bar{3}m$), and consists of the MO_2 layers with edge-sharing MO_6 octahedra. The edge-sharing structure allows the direct metal-metal bonding in addition to the indirect metal-oxygen-metal bonding, providing the rich electronic and magnetic properties [1,2]. Among them, LiCoO_2 is the very first system that has been employed in the pioneering work by Mizushima, Jones, Wiseman, and Goodenough [3], and has been one of the most important electrode materials for commercial Li-ion batteries [4–6]. Since Co is the least abundant element among the $3d$ transition metals and remains relatively expensive, alternative cathode materials with less expensive transition-metal elements have been developed [7,8]. It has been known that stability of the electrodes in the charge/discharge cycles is degraded if the Jahn-Teller active ions such as Mn^{3+} (high spin $t_{2g}^3e_g^1$) and Ni^{3+} (low

spin $t_{2g}^6e_g^1$) are involved. In this context, one of the most successful systems is $\text{Li}(\text{Ni}_{0.5}^{2+}\text{Mn}_{0.5}^{4+})_{1-x}\text{Co}_x^{3+}\text{O}_2$ including $\text{LiNi}_{0.5}^{2+}\text{Mn}_{0.5}^{4+}\text{O}_2$ as the end member ($x = 0.0$) [9–11]. In the case of $\text{LiNi}_{1/3}^{2+}\text{Mn}_{1/3}^{4+}\text{Co}_{1/3}^{3+}\text{O}_2$, in addition to the oxidation from Co^{3+} to Co^{4+} , the Ni^{2+} can be oxidized to Ni^{3+} or Ni^{4+} [12,13].

Interestingly, in the charging process of the Co-free $\text{LiNi}_{0.5}^{2+}\text{Mn}_{0.5}^{4+}\text{O}_2$, Ni^{2+} ejects two electrons and changes to Ni^{4+} avoiding the Jahn-Teller active low spin $t_{2g}^6e_g^1$ configuration [14]. From the core level spectroscopy, it has been known that the O $2p$ -to-Ni $3d$ charge-transfer energy is close to zero or even negative in Ni^{3+} oxides. Under the negative charge-transfer energy, the electronic configuration of Ni^{3+} becomes $d^8\bar{L}$ ($t_{2g}^6e_g^2\bar{L}$) rather than d^7 ($t_{2g}^6e_g^1$) where L represents an O $2p$ hole. Since the $3d$ orbitals with the e_g symmetry hybridize with the O $2p$ orbitals with the same symmetry in the NiO_6 octahedron, the $d^8\bar{L}$ state cannot avoid the Jahn-Teller instability. However, as pointed out by Mizokawa, Khomskii, and Sawatzky in 2000 [15], with the negative charge-transfer energy, the charge disproportionation $2\text{Ni}^{3+}(d^8\bar{L}) \rightarrow \text{Ni}^{2+}(d^8) + \text{Ni}^{4+}(d^8\bar{L}^2)$ can naturally occur by oxygen hole transfer avoiding the Jahn-Teller active $d^8\bar{L}$ state. In this scheme, the oxidation from Ni^{2+} to Ni^{4+} in the charging process of the $\text{LiNi}_{0.5}^{2+}\text{Mn}_{0.5}^{4+}\text{O}_2$ cathode can be understood in a systematic manner.

Soft x-ray spectroscopy is a powerful technique to study valence states of various $3d$ transition-metal oxides since

Published by the American Physical Society under the terms of the [Creative Commons Attribution 4.0 International license](https://creativecommons.org/licenses/by/4.0/). Further distribution of this work must maintain attribution to the author(s) and the published article's title, journal citation, and DOI. Open access publication funded by Max Planck Society.

x-ray absorption spectral shape at the transition-metal $2p$ core level exhibits specific multiplet structure [16–21]. Indeed, an x-ray absorption spectroscopy (XAS) study of $\text{LiNi}_{0.5}\text{Mn}_{0.5}\text{O}_2$ has confirmed that the Mn^{4+} and Ni^{2+} valence states manifest in the Mn $2p$ and Ni $2p$ x-ray absorption spectra [22]. Considering the difficulty of oxidation from Mn^{4+} to Mn^{5+} , Ni^{2+} should be oxidized to Ni^{3+} or Ni^{4+} although instability of $\text{Li}_x\text{Ni}_{0.5}\text{Mn}_{0.5}\text{O}_2$ in the ambient condition does not allow its soft x-ray absorption spectroscopy study. On the other hand, excess Li in $\text{Li}_{1+x}[\text{Ni}_{0.5}\text{Mn}_{0.5}]_{1-x}\text{O}_2$ introduces the Jahn-Teller active Mn^{3+} species and the resulting structural instability [23]. More recently, it has been revealed that LiNiO_2 harbors charge disproportionated states rather than the Jahn-Teller active Ni^{3+} state. Green *et al.* proposed a mechanism based on a Ni-O bond disproportionation which provides $\text{Ni}^{(2+\delta)+}/\text{Ni}^{(4-\delta)+}$ charge disproportionation (formally $\text{Ni}^{2+}/\text{Ni}^{4+}$ charge disproportionation) [24]. In more recent studies by Huang *et al.* and Wang *et al.* [25,26], calculations performed by C.-Y. Kuo were able to reproduce the spectra with a disproportionation of $\text{Ni}^{(2+\delta)+}/\text{Ni}^{(4-\delta)+}$, with $\delta \approx 0.4$. Both proposed models agree that the disproportionation, the intercluster hopping, and the charge transfer are crucial elements to explain the electronic structure of LiNiO_2 . This new insight on LiNiO_2 provides a clue for understanding the valence state in the delithiation process of $\text{LiNi}_{0.5}\text{Mn}_{0.5}\text{O}_2$ in which oxidation from Ni^{2+} to Ni^{3+} or Ni^{4+} is expected.

In the present work, we focus on the electronic structure of $\text{LiNi}_{1-x}\text{Co}_x\text{O}_2$ and $\text{Li}(\text{Ni}_{0.5}\text{Mn}_{0.5})_{1-x}\text{Co}_x\text{O}_2$ with the aim of getting a better and systematic understanding of the complex charge and valence behavior of LiMO_2 systems with Ni cations. We will present XAS measurements on $L_{2,3}$ edges of the transition metals to directly study their electronic structure and valencies, as well as on the O- K edge [27,28], which will provide a better insight on how the oxygen states contribute via the charge-transfer processes.

II. METHODS

Powder samples of $\text{LiNi}_{1-x}\text{Co}_x\text{O}_2$ and $\text{Li}(\text{Ni}_{0.5}\text{Mn}_{0.5})_{1-x}\text{Co}_x\text{O}_2$ were synthesized via coprecipitation and solid-state methods. In the first step, stoichiometric amounts of $\text{NiSO}_4 \cdot 6\text{H}_2\text{O}$ (Wako), $\text{CoSO}_4 \cdot 5\text{H}_2\text{O}$ (Wako), and $\text{MnSO}_4 \cdot 7\text{H}_2\text{O}$ (Wako) were dissolved into purified water with a total concentration of 2 mol L^{-1} for the transition-metal ions. Ammonium water and NH_4OH aqueous solution were dropped separately into the transition-metal solution to produce precipitates. During dropping of the base solution, the pH of the mixed solution was kept at ~ 11 . The precipitation solution was heated at 55°C and stirred at 800 rpm overnight. The precipitation solution was centrifuged at 3500 rpm, and then supernatant solution was removed. In the second step, the obtained precipitate was mixed with $\text{LiOH} \cdot \text{H}_2\text{O}$ powder (Wako) with 5% excess Li to compensate volatilization at high temperatures, and then pressed into a pellet. The resulting pellet was heated at 700°C for LiNiO_2 , 800°C for $\text{LiNi}_{1-x}\text{Co}_x\text{O}_2$ ($x = 0.25$ and 0.75), 850°C for $\text{LiNi}_{0.5}\text{Co}_{0.5}\text{O}_2$ and $\text{LiNi}_{0.5}\text{Mn}_{0.5}\text{O}_2$, and 900°C for $\text{Li}(\text{Ni}_{0.5}\text{Mn}_{0.5})_{1-x}\text{Co}_x\text{O}_2$ ($x = 1/3$ and $2/3$) for 10 h with a ramping rate of $5^\circ\text{C}/\text{min}$ under an O_2 flow.

The samples were cooled to room temperature and were immediately transferred to the Ar glove box. All processes were performed without exposure to air and all aqueous solution were degassed with Ar gas. Rietveld refinement for powder x-ray diffraction patterns confirms the successful synthesis of $\text{Li}(\text{Ni}_{0.5}\text{Mn}_{0.5})_{1-x}\text{Co}_x\text{O}_2$ and $\text{LiNi}_{1-x}\text{Co}_x\text{O}_2$ (see Supplemental Material [29]). Here we note that in the case of, e.g., LiNiO_2 , the obtained structural parameters are highly consistent with a stoichiometric composition [30].

The soft x-ray absorption spectroscopy (XAS) experiments at the transition-metal $L_{2,3}$ edges as well as the oxygen K edge of $\text{LiNi}_{1-x}\text{Co}_x\text{O}_2$ and $\text{Li}(\text{Ni}_{0.5}\text{Mn}_{0.5})_{1-x}\text{Co}_x\text{O}_2$ powder samples were performed at the beamline TPS 45A1 of the synchrotron radiation facility National Synchrotron Radiation Research Center (NSRRC) in Taiwan using the total electron yield (TEY) mode. All experiments were performed at 300 K and in ultrahigh-vacuum (UHV) conditions with base pressure of around 10^{-10} mbar. Single crystals of NiO, CoO, and MnO were measured simultaneously as an energy reference for the Ni, Co, and Mn $L_{2,3}$ edges, respectively. The powder samples were pressed onto carbon tape in an argon atmosphere inside a glove box and were briefly exposed to air for less than one minute during the loading of the samples into the loadlock of the UHV setup for the experiments.

III. RESULTS

A. $\text{Li}(\text{Ni}_{0.5}\text{Mn}_{0.5})_{1-x}\text{Co}_x\text{O}_2$

We start by studying the $\text{Ni}_{0.5}\text{Mn}_{0.5}$ -substitution system. Figure 1(a) shows the Co- $L_{2,3}$ XAS spectra of the $\text{Li}(\text{Ni}_{0.5}\text{Mn}_{0.5})_{1-x}\text{Co}_x\text{O}_2$ samples. Here in all cases we see almost identical spectra, which are similar also to the Co- $L_{2,3}$ of LiCoO_2 reported in previous studies [28,31]. The energy position as well as the intensities of the main spectral features display strong similarities to those of LaCoO_3 in its low-temperature phase [32], which is shown as an example of a Co^{3+} low-spin system, indicating that the Co^{3+} valence is kept in all displayed compositions. We observe some additional small features on the lower-energy side of the main absorption peak, indicating a small amount of Co^{2+} present in the samples. We will later show that the 2^+ signal most likely originates from surface reduction effects.

Next, we show in Fig. 1(b) the Mn- $L_{2,3}$ XAS spectra of the $\text{Li}(\text{Ni}_{0.5}\text{Mn}_{0.5})_{1-x}\text{Co}_x\text{O}_2$ samples. These spectra display features that are very similar in their shapes and energy positions to those of the SrMnO_3 , shown as an example of a Mn^{4+} system, confirming the Mn^{4+} valence for all cases in $\text{Li}(\text{Ni}_{0.5}\text{Mn}_{0.5})_{1-x}\text{Co}_x\text{O}_2$. For $x = 0.33$ and 0.66 , a small shoulder at 640 eV matching the strongest features of MnO suggests that a small amount of Mn^{2+} is also present in these samples.

Finally, Fig. 1(c) shows the Ni- $L_{2,3}$ XAS spectra of the $\text{Li}(\text{Ni}_{0.5}\text{Mn}_{0.5})_{1-x}\text{Co}_x\text{O}_2$ samples. The spectral shape strongly resembles in all cases that of the NiO, measured as a reference with Ni^{2+} , indicating a clear and stable 2^+ valence of the Ni.

We have thus established the stable Co^{3+} valence throughout all measured compositions of $\text{Li}(\text{Ni}_{0.5}\text{Mn}_{0.5})_{1-x}\text{Co}_x\text{O}_2$, as well as a stable Mn^{4+} and Ni^{2+} valence for the Mn and Ni ions in the $\text{Ni}_{0.5}\text{Mn}_{0.5}$ pairs. This is consistent with the behavior

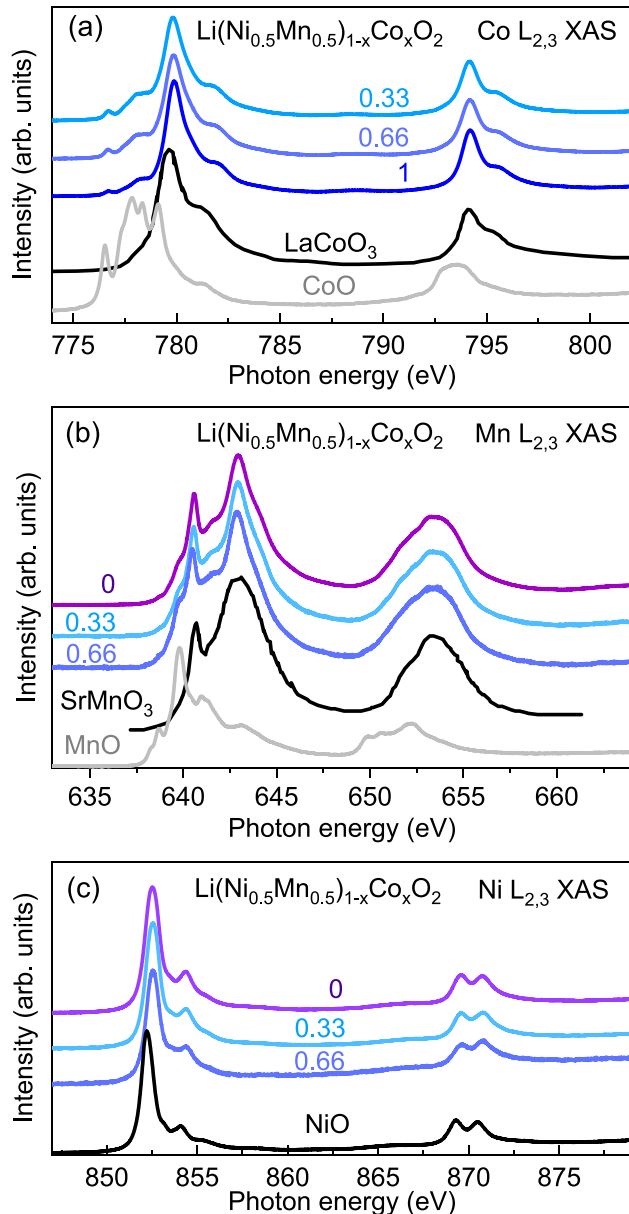


FIG. 1. Experimental transition-metal $L_{2,3}$ XAS spectra of the $\text{Li}(\text{Ni}_{0.5}\text{Mn}_{0.5})_{1-x}\text{Co}_x\text{O}_2$ samples, together with reference spectra of the respective transition metals. (a) Co- $L_{2,3}$ spectra, shown together with the spectra of LaCoO_3 (at its low-spin phase) as a Co^{3+} example (taken from [32]), and CoO as a Co^{2+} reference. (b) Mn- $L_{2,3}$ spectra, together with SrMnO_3 (Mn^{4+} , taken from [33]) and MnO (Mn^{2+}) as references. (c) Ni- $L_{2,3}$ spectra, together with NiO as a Ni^{2+} reference.

of the end member $\text{LiNi}_{0.5}\text{Mn}_{0.5}\text{O}_2$ already reported in the literature, and indicates that the concentration of Co does not alter the preference of having the $\text{Ni}^{2+}\text{Mn}^{4+}$ pairs. Therefore, the substitution of $\text{Ni}_{0.5}\text{Mn}_{0.5}$ results in the nominal 3^+ on average, rather than having the Jahn-Teller active Mn^{3+} and Ni^{3+} .

Next, we study the O-K edge in order to understand the behavior of the oxygen anions. Figure 2 presents O-K edge measurements of $\text{Li}(\text{Ni}_{0.5}\text{Mn}_{0.5})_{1-x}\text{Co}_x\text{O}_2$. For $x = 1$ (i.e., LiCoO_2), the O-K edge spectrum is comparable to previously reported results [31] and displays one strong single peak at

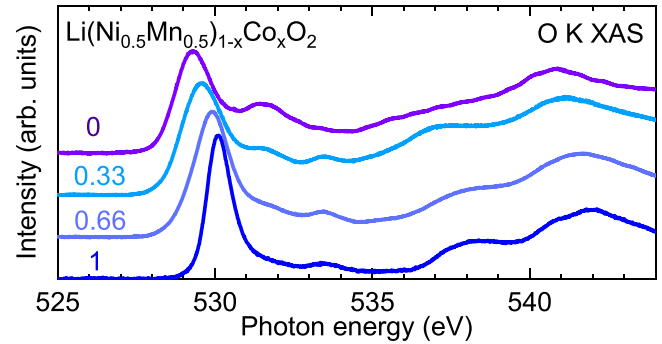


FIG. 2. Experimental O-K XAS spectra of the $\text{Li}(\text{Ni}_{0.5}\text{Mn}_{0.5})_{1-x}\text{Co}_x\text{O}_2$ samples.

around 530 eV from the hybridization of O $2p$ with the Co $3d(e_g)$ holes, as well as a small shoulder at 533.5 eV. This shoulder at 533.5 eV is also present in previous reports using TEY mode, but appears to be strongly suppressed when using the more bulk-sensitive fluorescence mode [31], hinting thus at its origin in the surface reduction of the sample/grains. We will provide further discussion later with the data from the $\text{LiNi}_{1-x}\text{Co}_x\text{O}_2$ system, where a larger peak is also observed at the same energy. With decreasing x we observe that the main peak shifts toward lower energies, as can be expected from the higher valency of the Mn^{4+} hybridizing with O $2p$. Furthermore, the peak becomes broader, as in this case O $2p$ can hybridize both with $\text{Mn}^{4+} e_g$ as well as t_{2g} states, resulting in extra structure in the O-K edge spectra originating from the crystal field splitting. Finally, we note that the surface reduction peak shifts toward lower energies with lower x , from 533.3 eV to 532.6 eV, because of the difference in the Mn^{4+} and Co^{3+} reduced states.

B. $\text{LiNi}_{1-x}\text{Co}_x\text{O}_2$

Now we study the $\text{LiNi}_{1-x}\text{Co}_x\text{O}_2$ system. Figure 3(a) shows the Co- $L_{2,3}$ XAS spectra of the $\text{LiNi}_{1-x}\text{Co}_x\text{O}_2$ samples. Similar to the $\text{Li}(\text{Ni}_{0.5}\text{Mn}_{0.5})_{1-x}\text{Co}_x\text{O}_2$ shown in Fig. 1(a), here for all compositions we observe a very similar spectral shape that is consistent with a Co^{3+} low-spin system. Here too, small traces of Co^{2+} from the surface reduction are present.

In the Ni- $L_{2,3}$ XAS spectra of $\text{LiNi}_{1-x}\text{Co}_x\text{O}_2$ [Fig. 3(b)], however, we observe significant changes with composition. Instead of having a single peak similar to NiO , we observe a doubling of the main peak at around 852–855 eV, which is analogous to that in many of the nominally Ni^{3+} systems [34–37]. The spectra obtained for $x = 0$ (i.e., LiNiO_2) is similar to other measurements on powder samples reported in the literature [24,38]. Comparing the results to either measurements using inverse partial fluorescent yield, which provides higher probing depth [24], or on single crystals [25], the low-energy peak at around 852.5 eV is significantly larger, indicating that the Ni^{2+} contamination is likely mainly present on the powder grain surface. We will later argue that this is consistent with the surface reduction feature present in the O-K edge in Fig. 4. Nevertheless, we can still observe a very clear peak splitting of around 2 eV. This large splitting is related to the charge disproportionation seen in such nominally

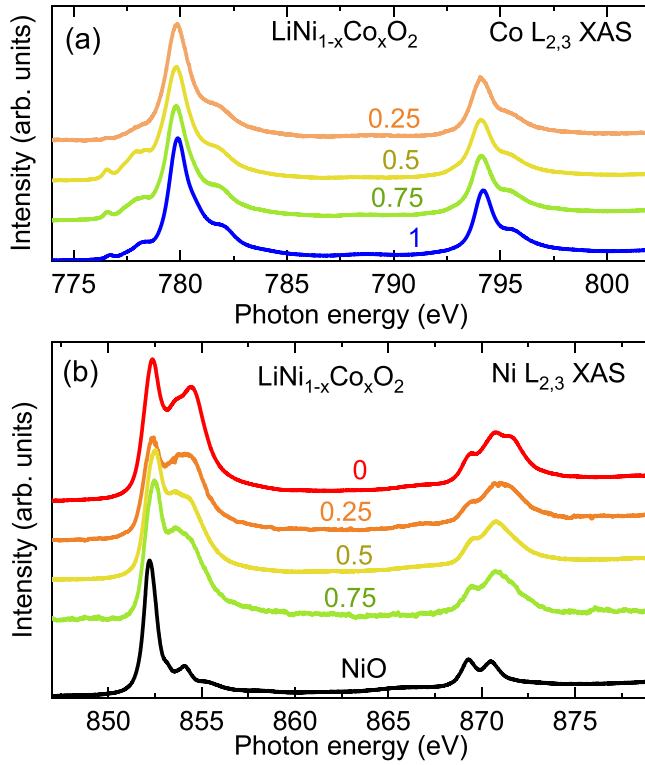


FIG. 3. Experimental transition-metal $L_{2,3}$ XAS spectra of the $\text{LiNi}_{1-x}\text{Co}_x\text{O}_2$ samples. (a) $\text{Co-}L_{2,3}$ spectra, and (b) $\text{Ni-}L_{2,3}$ spectra, together with NiO as a Ni^{2+} reference.

Ni^{3+} perovskites [39,40] including for LiNiO_2 [24,26,41], where the bond disproportionated $\text{Ni}^{(2+\delta)+}/\text{Ni}^{(4-\delta)+}$ ground state is given by the hybridization between multiple electronic configurations including $d^8-d^8\bar{L}^2$, $d^8-d^7\bar{L}$, d^8-d^6 , etc. ($\text{Ni}^{(2+\delta)+}$ for the longer Ni-O bond and $\text{Ni}^{(4-\delta)+}$ for the shorter Ni-O bond), rather than by a pure, single-site d^7 or $d^8\bar{L}$ configuration. By increasing x , the peak splitting is gradually closed, with the higher-energy peak shifting toward lower energies and smearing out, indicating that the intersite hopping allowing such disproportionations to occur is also gradually reduced [40]. In particular, we note that at higher values of x , the peak's shape appears similar to that of NaNiO_2 , better

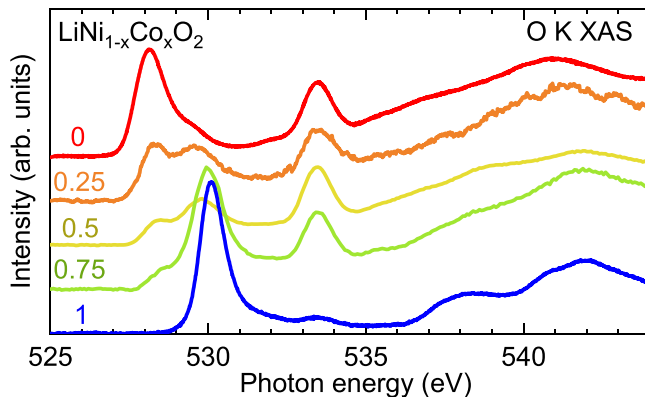


FIG. 4. Experimental O- K XAS spectra of the $\text{LiNi}_{1-x}\text{Co}_x\text{O}_2$ samples.

described by the Jahn-Teller distorted $d^8\bar{L}$ rather than by the bond disproportionated $\text{Ni}^{(2+\delta)+}/\text{Ni}^{(4-\delta)+}$, as it is in LiNiO_2 [24].

Figure 4 presents O- K edge measurements of $\text{LiNi}_{1-x}\text{Co}_x\text{O}_2$. For $x = 0$ we observe mainly two features: a large pre-peak at around 528 eV and a higher-energy peak at around 533.5 eV. This LiNiO_2 spectrum is comparable to that previously reported [24,42], with a strong pre-peak from the holes in the O $2p$ states resulting from the hybridization between Ni and O, and the higher-energy peak from the surface reduction, similar to the reduction peak observed in $\text{Li}(\text{Ni}_{0.5}\text{Mn}_{0.5})_{1-x}\text{Co}_x\text{O}_2$ in Fig. 2. The weight ratio between the pre-peak and the reduction peak is most comparable to results from sintered samples fractured on vacuum [24], indicating that the short exposure to air during the loading process has not affected the quality of the measured samples. Nevertheless, we note that the surface reduction peak at 533.5 eV is significantly larger than that observed in LiNiO_2 single crystals [25], likely meaning that this reduction already occurs at the surface of each powder grain regardless of its exposure to air. We observe that the intensity of this peak does indeed correlate to the amount of reduction on the transition-metal site: In $\text{LiNi}_{1-x}\text{Co}_x\text{O}_2$, where a sizable reduction peak is present, a more significant amount of Ni^{2+} signal seems to be present [Fig. 3(b)] as compared to the $\text{Li}(\text{Ni}_{0.5}\text{Mn}_{0.5})_{1-x}\text{Co}_x\text{O}_2$ systems where both the reduction peak and the signals from the reduced Mn^{2+} and Co^{2+} were much less pronounced (Fig. 1). As for the significantly low energy of the pre-peak compared to the main peak observed in the $\text{Li}(\text{Ni}_{0.5}\text{Mn}_{0.5})_{1-x}\text{Co}_x\text{O}_2$ series, it is indicative of the much lower charge-transfer energy at the Ni system, consistent with the negative charge-transfer character often observed in such nominally 3^+ nickelates. With increasing x we observe that the weight shifts from the peak at 528 eV to the one at 530 eV. We note here in particular that this weight shift occurs nonlinearly with x , indicating some additional cause beyond the direct Ni-Co ratio change, as we will discuss in detail later.

IV. DISCUSSION

For $\text{Li}(\text{Ni}_{0.5}\text{Mn}_{0.5})_{1-x}\text{Co}_x\text{O}_2$ in all compositions, the Co^{3+} , Ni^{2+} , and Mn^{4+} valencies are stable, with no significant differences observed in their spectra. In contrast to what is observed in the $\text{LiNi}_{1-x}\text{Co}_x\text{O}_2$ series, the Ni valence is stabilized to 2^+ due to the preference of Mn for being 4^+ . Furthermore, in all systems from this series only very small amounts of reduction are observed (both via the O- K edge and the transition-metal $L_{2,3}$ edges), suggesting the stability of the valencies also near the surface and grain boundaries.

As for the $\text{LiNi}_{1-x}\text{Co}_x\text{O}_2$ system, the Co is consistently 3^+ , but the Ni, which nominally would be 3^+ , shows significant changes. The much lower energy of the O- K pre-peak is consistent with a negative charge-transfer scenario, and furthermore the Ni- $L_{2,3}$ edges show signatures of charge disproportionation, making it similar to many systems with nominally Ni^{3+} .

The signature of the disproportionation on the Ni- $L_{2,3}$ edge is gradually reduced with increasing Co concentration, which can be understood as that the presence of Co ions would

disturb the most optimal disproportionation arrangements. The probability for the NiO_6 to be fully surrounded by other NiO_6 octahedra will decrease, which will inevitably favor a directionality, and thus, a Jahn-Teller mechanism instead of the (homogeneous) bond disproportionation. With increasing Co concentration we also observed a faster than linear decay with x of the low-energy pre-peak in the O- K spectra (i.e., beyond the pure stoichiometry change), suggesting the role of the disproportionation on the number of holes per Ni site.

The present observation is consistent with the oxidation from Ni^{2+} to Ni^{4+} in the delithiation process of $\text{LiMn}_{0.5}\text{Ni}_{0.5}\text{O}_2$. In $\text{Li}_{0.5}\text{Mn}_{0.5}\text{Ni}_{0.5}\text{O}_2$, Ni valence is disproportionated into $2^+(d^8)$ and $4^+(d^8L^2)$ rather than $3^+(d^8L)$. With increasing Co content, the charge disproportionation tends to be suppressed. In the delithiation process of $\text{LiMn}_{1/3}\text{Ni}_{1/3}\text{Co}_{1/3}\text{O}_2$, $\text{Ni}^{3+}(d^8L)$ may appear due to the Co^{3+} species. Most probably, the oxygen hole of $\text{Ni}^{4+}(d^8L^2)$ is partially taken by Co^{3+} . This oxygen hole transfer process corresponds to $\text{Ni}^{4+}(d^8L^2) + \text{Co}^{3+}(d^6) \rightarrow \text{Ni}^{3+}(d^8L) + \text{Co}^{4+}(d^6L)$.

Finally, the presence of significantly large reductions compared to the $\text{Li}(\text{Ni}_{0.5}\text{Mn}_{0.5})_{1-x}\text{Co}_x\text{O}_2$ systems as observed both on the O- K edge and the Ni- $L_{2,3}$ edge already indicates that the nominal 3^+ on the Ni is not too stable, instead preferring to reduce near the surface to become Ni^{2+} .

V. CONCLUSION

We performed a systematic study on the valence of the transition-metal ions in $\text{LiNi}_{1-x}\text{Co}_x\text{O}_2$ and $\text{Li}(\text{Ni}_{0.5}\text{Mn}_{0.5})_{1-x}\text{Co}_x\text{O}_2$ using the x-ray absorption spectra

of the transition-metal $L_{2,3}$ edges as well as the O- K edge. We showed that in $\text{Li}(\text{Ni}_{0.5}\text{Mn}_{0.5})_{1-x}\text{Co}_x\text{O}_2$ we have for all compositions Co^{3+} together with $\text{Mn}_{0.5}^{4+}\text{-Ni}_{0.5}^{2+}$. Only a small amount of reduction can be observed both in the $L_{2,3}$ as well as in O- K edges, suggesting its stability even close to the grain boundaries and surfaces. The $\text{LiNi}_{1-x}\text{Co}_x\text{O}_2$ however displays a more complex behavior. The Co is here also 3^+ , forcing the Ni to be nominally also in a 3^+ state, resulting in a charge disproportionate negative charge transfer system as often occurring in compounds containing such nominally Ni^{3+} . For higher concentrations of Co, the disproportionation signal decreases, with the number of O $2p$ holes also decreasing, resulting in a more intricate but unstable behavior. In particular, the nominal Ni^{3+} gives the system greater propensity to reductions in the surface.

ACKNOWLEDGMENTS

D.T. acknowledges support by the Deutsche Forschungsgemeinschaft (DFG, German Research Foundation) under the Walter Benjamin Programme, Project No. 521584902. We acknowledge support for the measurements from the Max Planck-POSTECH-Hsinchu Center for Complex Phase Materials. M.C. benefited from the support of the German Research Foundation (DFG), Project No. 387555779. M.O. is financially supported by Grant-in-Aid for Scientific Research (A) No. 21H04697, Grant-in-Aid for Scientific Research on Innovative Areas No. 19H05816, the Ministry of Education, Culture, Sports, Science, and Technology (MEXT) Program (Grant No. JPMXP1121467561), and JST CREST Grant No. JPMJCR2106.

-
- [1] J. B. Goodenough, *Magnetism and the Chemical Bond* (Interscience, New York, 1963).
 - [2] D. I. Khomskii, *Transition Metal Compounds* (Cambridge University Press, Cambridge, 2014).
 - [3] K. Mizushima, P. Jones, P. Wiseman, and J. Goodenough, *Mater. Res. Bull.* **15**, 783 (1980).
 - [4] E. Plichta, S. Slane, M. Uchiyama, M. Salomon, D. Chua, W. B. Ebner, and H. W. Lin, *J. Electrochem. Soc.* **136**, 1865 (1989).
 - [5] H. Gibbard, *J. Power Sources* **26**, 81 (1989).
 - [6] T. Nagaura and K. Tozawa, *Prog. Batt. Solar Cells* **2**, 209 (1990).
 - [7] S.-T. Myung, F. Maglia, K.-J. Park, C. S. Yoon, P. Lamp, S.-J. Kim, and Y.-K. Sun, *ACS Energy Lett.* **2**, 196 (2017).
 - [8] M. Bianchini, M. Roca-Ayats, P. Hartmann, T. Brezesinski, and J. Janek, *Angew. Chem. Int. Ed.* **58**, 10434 (2019).
 - [9] T. Ohzuku and Y. Makimura, *Chem. Lett.* **30**, 744 (2001).
 - [10] Z. Lu, D. D. MacNeil, and J. R. Dahn, *Electrochem. Solid-State Lett.* **4**, A200 (2001).
 - [11] B. L. Cushing and J. B. Goodenough, *Solid State Sci.* **4**, 1487 (2002).
 - [12] W.-S. Yoon, M. Balasubramanian, K. Y. Chung, X.-Q. Yang, J. McBreen, C. P. Grey, and D. A. Fischer, *J. Am. Chem. Soc.* **127**, 17479 (2005).
 - [13] Y. W. Tsai, B. J. Hwang, G. Ceder, H. S. Sheu, D. G. Liu, and J. F. Lee, *Chem. Mater.* **17**, 3191 (2005).
 - [14] Y. Idemoto, T. Hasegawa, N. Kitamura, and Y. Uchimoto, *Electrochemistry* **79**, 15 (2011).
 - [15] T. Mizokawa, D. I. Khomskii, and G. A. Sawatzky, *Phys. Rev. B* **61**, 11263 (2000).
 - [16] F. M. F. de Groot, J. C. Fuggle, B. T. Thole, and G. A. Sawatzky, *Phys. Rev. B* **42**, 5459 (1990).
 - [17] F. M. F. de Groot, *J. Electron Spectrosc. Relat. Phenom.* **67**, 529 (1994).
 - [18] F. de Groot and A. Kotani, *Core Level Spectroscopy of Solids* (CRC Press, Boca Raton, 2014).
 - [19] H. Wu, T. Burnus, Z. Hu, C. Martin, A. Maignan, J. C. Cezar, A. Tanaka, N. B. Brookes, D. I. Khomskii, and L. H. Tjeng, *Phys. Rev. Lett.* **102**, 026404 (2009).
 - [20] C. F. Chang, Z. Hu, S. Klein, X. H. Liu, R. Sutarto, A. Tanaka, J. C. Cezar, N. B. Brookes, H.-J. Lin, H. H. Hsieh, C. T. Chen, A. D. Rata, and L. H. Tjeng, *Phys. Rev. X* **6**, 041011 (2016).
 - [21] D. Takegami, Z. Hu, J. Falke, A. Meléndez-Sans, C.-E. Liu, C.-F. Chang, C.-Y. Kuo, C.-T. Chen, H. Guo, A. Komarek, A. Tanaka, S. Hébert, and L. H. Tjeng, *Z. Anorg. Allg. Chem.* **649**, e202300077 (2023).

- [22] H. Wadati, D. G. Hawthorn, T. Z. Regier, G. Chen, T. Hitosugi, T. Mizokawa, A. Tanaka, and G. A. Sawatzky, *Appl. Phys. Lett.* **97**, 022106 (2010).
- [23] Y. Yokoyama, D. Ootsuki, T. Sugimoto, H. Wadati, J. Okabayashi, X. Yang, F. Du, G. Chen, and T. Mizokawa, *Appl. Phys. Lett.* **107**, 033903 (2015).
- [24] R. J. Green, H. Wadati, T. Z. Regier, A. J. Achkar, C. McMahon, J. P. Clancy, H. A. Dabkowska, B. D. Gaulin, G. A. Sawatzky, and D. G. Hawthorn, Evidence for bond disproportionation in LiNiO₂ from x-ray absorption spectroscopy, [arXiv:2011.06441](https://arxiv.org/abs/2011.06441).
- [25] H. Huang, Y.-C. Chang, Y.-C. Huang, L. Li, A. C. Komarek, L. H. Tjeng, Y. Orikasa, C.-W. Pao, T.-S. Chan, J.-M. Chen, S.-C. Haw, J. Zhou, Y. Wang, H.-J. Lin, C.-T. Chen, C.-L. Dong, C.-Y. Kuo, J.-Q. Wang, Z. Hu, and L. Zhang, *Nat. Commun.* **14**, 2112 (2023).
- [26] L. Wang, A. Mukherjee, C.-Y. Kuo, S. Chakrabarty, R. Yemini, A. A. Dameron, J. W. DuMont, S. H. Akella, A. Saha, S. Taragin, H. Aviv, D. Naveh, D. Sharon, T.-S. Chan, H.-J. Lin, J.-F. Lee, C.-T. Chen, B. Liu, X. Gao, S. Basu *et al.*, *Nat. Nanotechnol.* **19**, 208 (2024).
- [27] F. M. F. de Groot, M. Grioni, J. C. Fuggle, J. Ghijsen, G. A. Sawatzky, and H. Petersen, *Phys. Rev. B* **40**, 5715 (1989).
- [28] T. Mizokawa, Y. Wakisaka, T. Sudayama, C. Iwai, K. Miyoshi, J. Takeuchi, H. Wadati, D. G. Hawthorn, T. Z. Regier, and G. A. Sawatzky, *Phys. Rev. Lett.* **111**, 056404 (2013).
- [29] See Supplemental Material at <http://link.aps.org/supplemental/10.1103/PhysRevMaterials.8.055401> for the structural characterization of the measured samples.
- [30] H. Li, N. Zhang, J. Li, and J. R. Dahn, *J. Electrochem. Soc.* **165**, A2985 (2018).
- [31] C.-H. Chen, B.-J. Hwang, C.-Y. Chen, S.-K. Hu, J.-M. Chen, H.-S. Sheu, and J.-F. Lee, *J. Power Sources* **174**, 938 (2007).
- [32] M. W. Haverkort, Z. Hu, J. C. Cezar, T. Burnus, H. Hartmann, M. Reuther, C. Zobel, T. Lorenz, A. Tanaka, N. B. Brookes, H. H. Hsieh, H.-J. Lin, C. T. Chen, and L. H. Tjeng, *Phys. Rev. Lett.* **97**, 176405 (2006).
- [33] T. Burnus, Z. Hu, H. H. Hsieh, V. L. J. Joly, P. A. Joy, M. W. Haverkort, H. Wu, A. Tanaka, H.-J. Lin, C. T. Chen, and L. H. Tjeng, *Phys. Rev. B* **77**, 125124 (2008).
- [34] T. Mizokawa, A. Fujimori, T. Arima, Y. Tokura, N. Mōri, and J. Akimitsu, *Phys. Rev. B* **52**, 13865 (1995).
- [35] C. Piamonteze, F. M. F. de Groot, H. C. N. Tolentino, A. Y. Ramos, N. E. Massa, J. A. Alonso, and M. J. Martínez-Lope, *Phys. Rev. B* **71**, 020406(R) (2005).
- [36] H. Guo, Z. W. Li, L. Zhao, Z. Hu, C. F. Chang, C.-Y. Kuo, W. Schmidt, A. Piovano, T. W. Pi, O. Sobolev, D. I. Khomskii, L. H. Tjeng, and A. C. Komarek, *Nat. Commun.* **9**, 43 (2018).
- [37] H. Guo, Z. W. Li, C. F. Chang, Z. Hu, C.-Y. Kuo, T. G. Perring, W. Schmidt, A. Piovano, K. Schmalzl, H. C. Walker, H. J. Lin, C. T. Chen, S. Blanco-Canosa, J. Schlappa, C. Schüßler-Langeheine, P. Hansmann, D. I. Khomskii, L. H. Tjeng, and A. C. Komarek, *Sci. Rep.* **10**, 18012 (2020).
- [38] Y. Ren, R. Yamaguchi, T. Uchiyama, Y. Orikasa, T. Watanabe, K. Yamamoto, T. Matsunaga, Y. Nishiki, S. Mitsushima, and Y. Uchimoto, *ChemElectroChem* **8**, 70 (2021).
- [39] S. Johnston, A. Mukherjee, I. Elfimov, M. Berciu, and G. A. Sawatzky, *Phys. Rev. Lett.* **112**, 106404 (2014).
- [40] R. J. Green, M. W. Haverkort, and G. A. Sawatzky, *Phys. Rev. B* **94**, 195127 (2016).
- [41] K. Foyevtsova, I. Elfimov, J. Rottler, and G. A. Sawatzky, *Phys. Rev. B* **100**, 165104 (2019).
- [42] P. Kuiper, G. Kruizinga, J. Ghijsen, G. A. Sawatzky, and H. Verweij, *Phys. Rev. Lett.* **62**, 221 (1989).